

Supplementary Information

**Reactive species specific RhB assisted collective photocatalytic degradation of tetracycline antibiotic with triple-layer Aurivillius perovskites**

Jaideep Malik,<sup>a</sup> Shubham Kumar,<sup>a</sup> and Tapas Kumar Mandal<sup>a,b,\*</sup>

<sup>a</sup>Department of Chemistry & <sup>b</sup>Centre of Nanotechnology, Indian Institute of Technology Roorkee, Roorkee – 247 667, India.

E-mail: tapas.mandal@cy.iitr.ac.in.

Compounds	Lattice parameters (Å)		Bandgap (eV)		Table S1 Unit cell parameters and bandga
	<i>a</i>	<i>c</i>	<i>E<sub>g</sub></i> (1)	<i>E<sub>g</sub></i> (2)	
Bi <sub>2.5</sub> Sr <sub>1.5</sub> Nb <sub>2</sub> Ti <sub>0.5</sub> Cr <sub>0.5</sub> O <sub>12</sub>	3.886(1)	33.04(1)	1.94	2.28	
Bi <sub>2.5</sub> Sr <sub>1.5</sub> Nb <sub>2</sub> Ti <sub>0.5</sub> Mn <sub>0.5</sub> O <sub>12</sub>	3.884(1)	32.99(1)	1.69	3.11	
Bi <sub>2.5</sub> Sr <sub>1.5</sub> Nb <sub>2</sub> Ti <sub>0.5</sub> Fe <sub>0.5</sub> O <sub>12</sub>	3.895(1)	33.21(1)	2.16	2.75	

p of Bi<sub>2.5</sub>Sr<sub>1.5</sub>Nb<sub>2</sub>Ti<sub>0.5</sub>M<sub>0.5</sub>O<sub>12</sub> (M = Cr, Mn, Fe)

Atom	x	y	z	B <sub>iso</sub>	Occ.
Bi(1)/Sr(1)	0	0	0.21379(6)	4.5	1.8/0.2
Sr(2)/Bi(2)	0	0	0.06313(9)	2.5	1.3/0.7
Ti(1)/Nb(1)/Fe(1)	0	0	0.5	0.9	0.25/0.5/0.25
Nb(2)/Ti(2)/Fe(2)	0	0	0.37268(7)	0.6	1.5/0.25/0.25
O(1)	0	0.5	0	4.4	2
O(2)	0	0.5	0.25	2.0	2
O(3)	0	0	0.44662(52)	2.0	2
O(4)	0	0	0.32157(62)	3.6	2
O(5)	0	0.5	0.11590(38)	1.5	4

**Table S2.** Atomic Position, Site Occupancy and Thermal Parameters of  $\text{Bi}_{2.5}\text{Sr}_{1.5}\text{Nb}_2\text{Ti}_{0.5}\text{Cr}_{0.5}\text{O}_{12}$

Space group  $I4/mmm$ ,  $a = 3.8949(2)$ ,  $c = 33.040(2)$  Å,  $R_{\text{Bragg}} = 5.1$  %,  $R_{\text{F}} = 2.0$  %,  $R_{\text{p}} = 8.1$  %,  $R_{\text{wp}} = 10.0$  % and  $\chi^2 = 7.9$ .

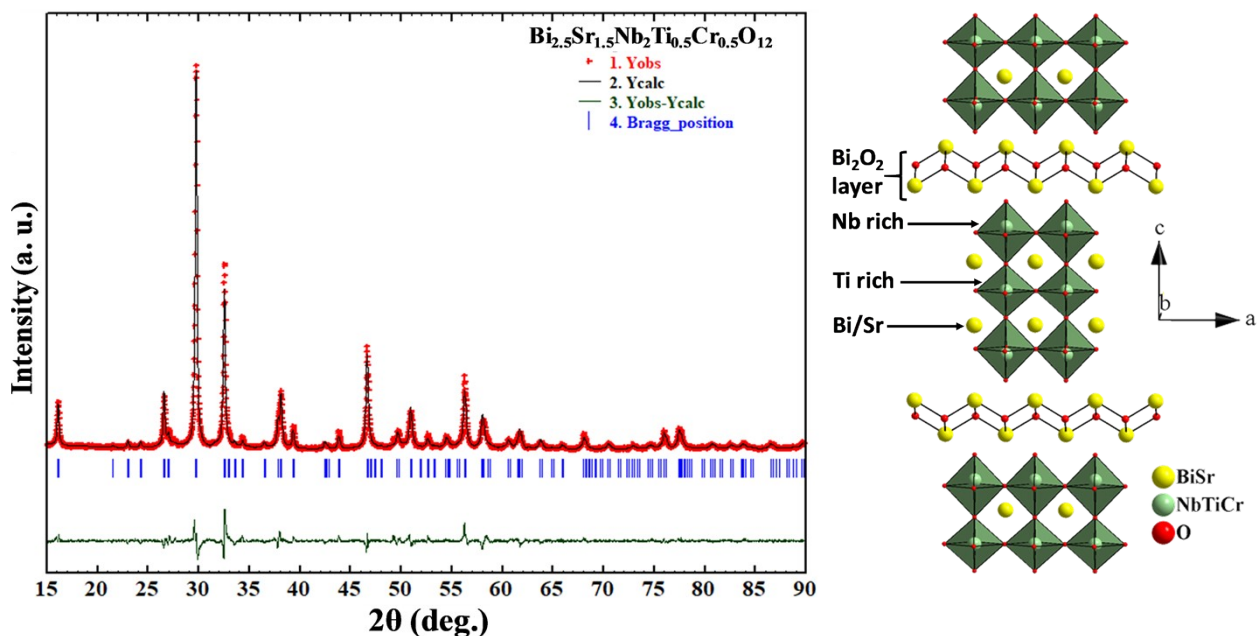


**Fig. S1** Rietveld refinement profile of  $\text{Bi}_{2.5}\text{Sr}_{1.5}\text{Nb}_2\text{Ti}_{0.5}\text{Cr}_{0.5}\text{O}_{12}$  (left panel). Observed (+), calculated (–) and difference (bottom) profiles are shown with vertical bars representing Bragg positions. The crystal structure of  $\text{Bi}_{2.5}\text{Sr}_{1.5}\text{Nb}_2\text{Ti}_{0.5}\text{Cr}_{0.5}\text{O}_{12}$  is represented in the right panel.

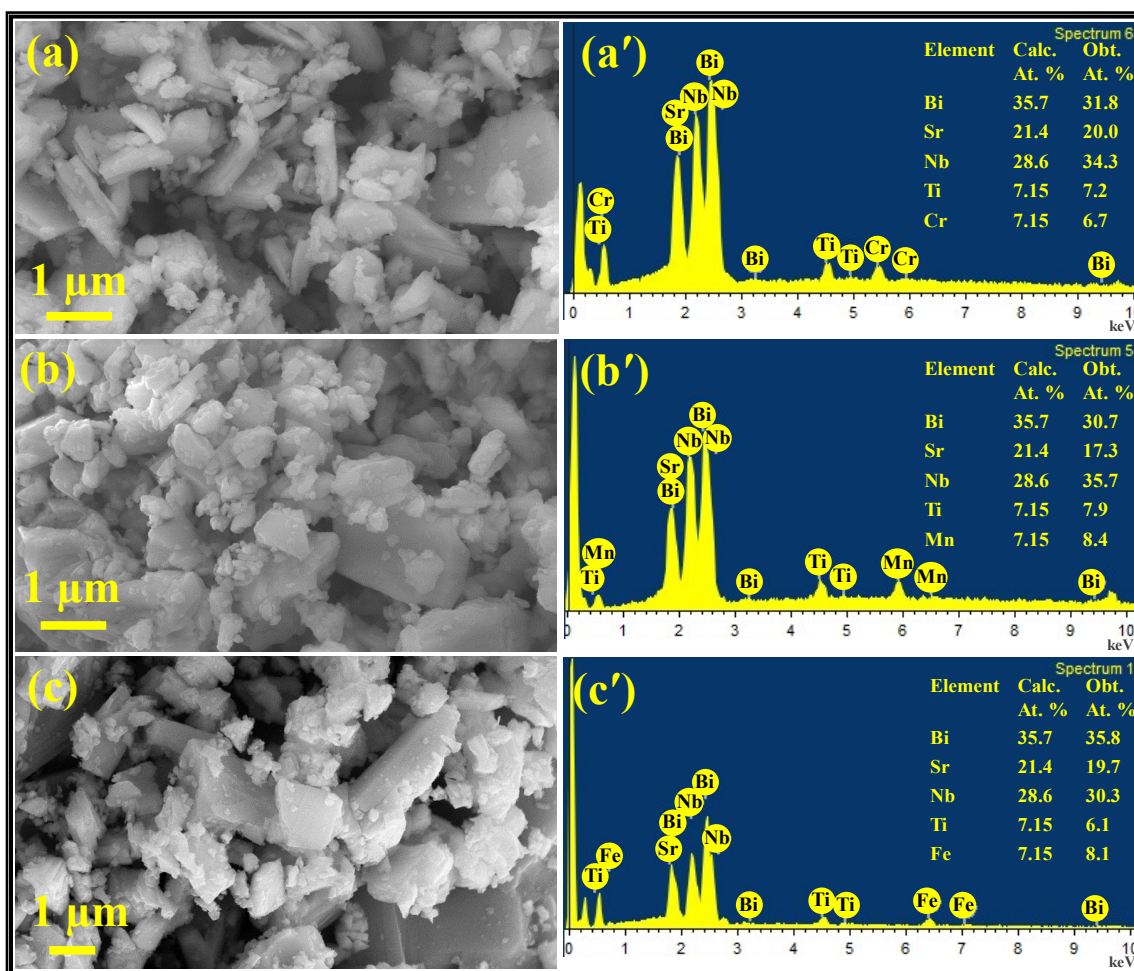


**Fig. S2** FE-SEM images and corresponding EDS of (a, a')  $\text{Bi}_{2.5}\text{Sr}_{1.5}\text{Nb}_2\text{Ti}_{0.5}\text{Cr}_{0.5}\text{O}_{12}$ , (b, b')  $\text{Bi}_{2.5}\text{Sr}_{1.5}\text{Nb}_2\text{Ti}_{0.5}\text{Mn}_{0.5}\text{O}_{12}$  and (c, c')  $\text{Bi}_{2.5}\text{Sr}_{1.5}\text{Nb}_2\text{Ti}_{0.5}\text{Fe}_{0.5}\text{O}_{12}$ .

**Table S3.** The specific surface area & pore diameter of  $\text{Bi}_{2.5}\text{Sr}_{1.5}\text{Nb}_2\text{Ti}_{0.5}\text{M}_{0.5}\text{O}_{12}$  (M = Cr, Mn & Fe)

Photocatalyst	Surface area (m <sup>2</sup> /g)	Pore diameter (nm)
Bi <sub>2.5</sub> Sr <sub>1.5</sub> Nb <sub>2</sub> Ti <sub>0.5</sub> Cr <sub>0.5</sub> O <sub>12</sub>	1.3386	14.74
Bi <sub>2.5</sub> Sr <sub>1.5</sub> Nb <sub>2</sub> Ti <sub>0.5</sub> Mn <sub>0.5</sub> O <sub>12</sub>	1.2844	14.56
Bi <sub>2.5</sub> Sr <sub>1.5</sub> Nb <sub>2</sub> Ti <sub>0.5</sub> Fe <sub>0.5</sub> O <sub>12</sub>	1.1831	14.43

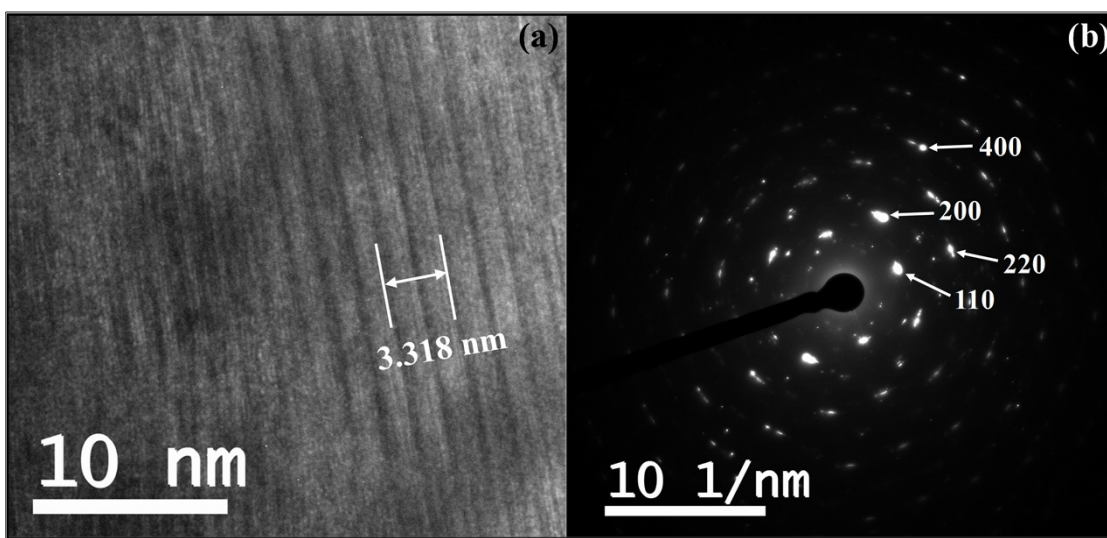


Fig. S3 (a) HR-TEM image and (b) SAED pattern of Bi<sub>2.5</sub>Sr<sub>1.5</sub>Nb<sub>2</sub>Ti<sub>0.5</sub>Fe<sub>0.5</sub>O<sub>12</sub>.

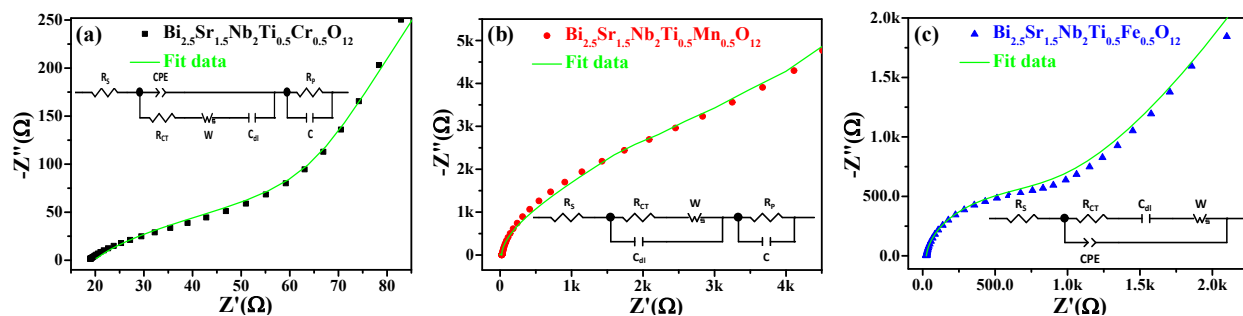
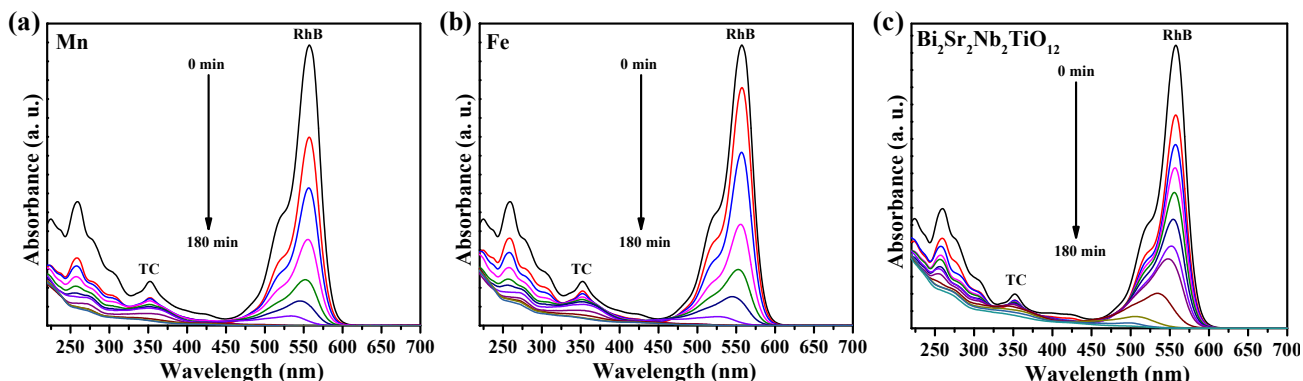
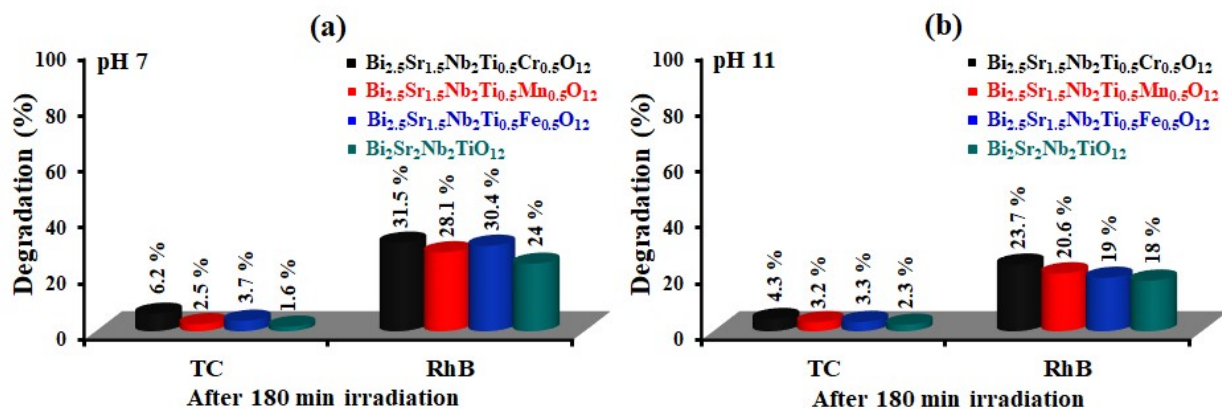


Fig. S4 Nyquist plot fitting and equivalent circuit diagram for Bi<sub>2.5</sub>Sr<sub>1.5</sub>Nb<sub>2</sub>Ti<sub>0.5</sub>M<sub>0.5</sub>O<sub>12</sub> (M = Cr, Mn & Fe).



**Fig. S5** UV-vis spectra showing collective degradation of TC and RhB with MP-MVL irradiation over  $\text{Bi}_{2.5}\text{Sr}_{1.5}\text{Nb}_2\text{Ti}_{0.5}\text{M}_{0.5}\text{O}_{12}$  ( $M = \text{Mn}$  &  $\text{Fe}$ ) and  $\text{Bi}_2\text{Sr}_2\text{Nb}_2\text{TiO}_{12}$ .



**Fig. S6** Photocatalytic degradation of TC and RhB from TC-RhB mixture over  $\text{Bi}_{2.5}\text{Sr}_{1.5}\text{Nb}_2\text{Ti}_{0.5}\text{M}_{0.5}\text{O}_{12}$  ( $M = \text{Cr}$ ,  $\text{Mn}$ ,  $\text{Fe}$ ) and  $\text{Bi}_2\text{Sr}_2\text{Nb}_2\text{TiO}_{12}$  at (a) pH 7 and (b) pH 11.

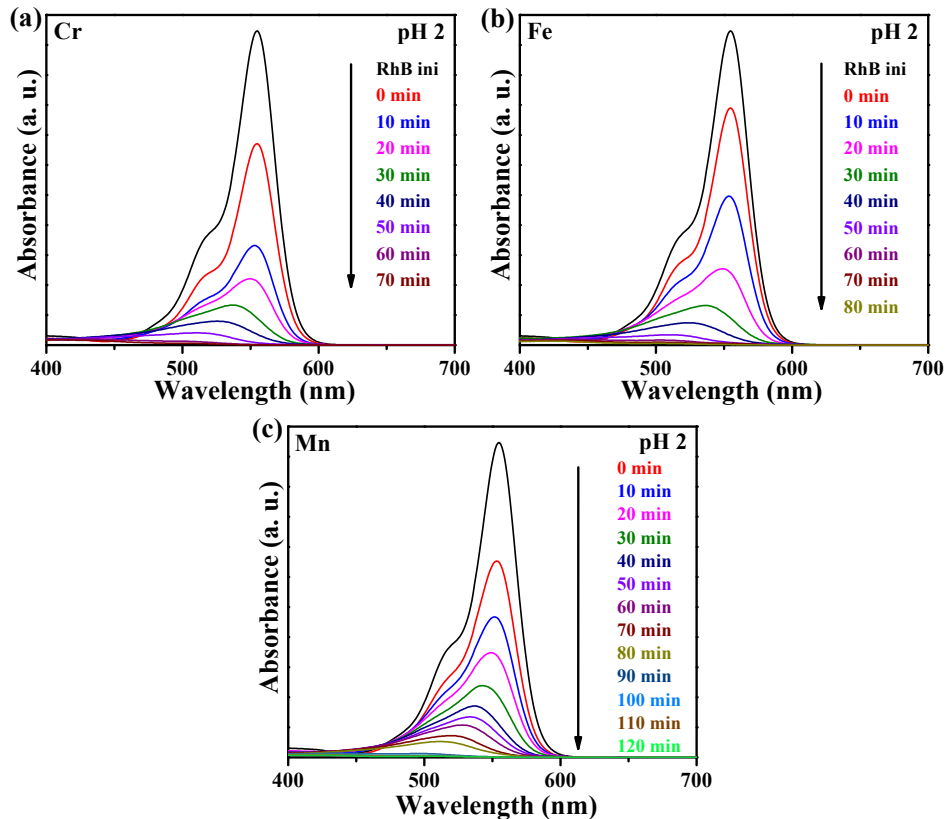


**Fig. S7** UV-vis absorption spectra for degradation of RhB over (a)  $\text{Bi}_{2.5}\text{Sr}_{1.5}\text{Nb}_2\text{Ti}_{0.5}\text{Cr}_{0.5}\text{O}_{12}$ , (b)  $\text{Bi}_{2.5}\text{Sr}_{1.5}\text{Nb}_2\text{Ti}_{0.5}\text{Mn}_{0.5}\text{O}_{12}$  and (c)  $\text{Bi}_{2.5}\text{Sr}_{1.5}\text{Nb}_2\text{Ti}_{0.5}\text{Fe}_{0.5}\text{O}_{12}$  at pH 2 under MP-MVL irradiation.

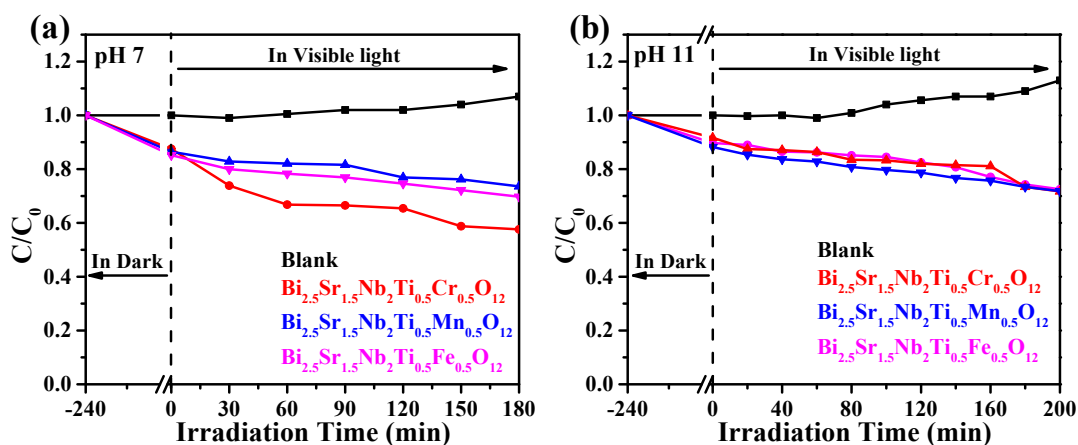


**Fig. S8** Photocatalytic degradation of RhB with time over  $\text{Bi}_{2.5}\text{Sr}_{1.5}\text{Nb}_2\text{Ti}_{0.5}\text{M}_{0.5}\text{O}_{12}$  ( $M = \text{Cr}, \text{Mn}, \text{Fe}$ ) at (a) pH 7 and (b) pH 11.

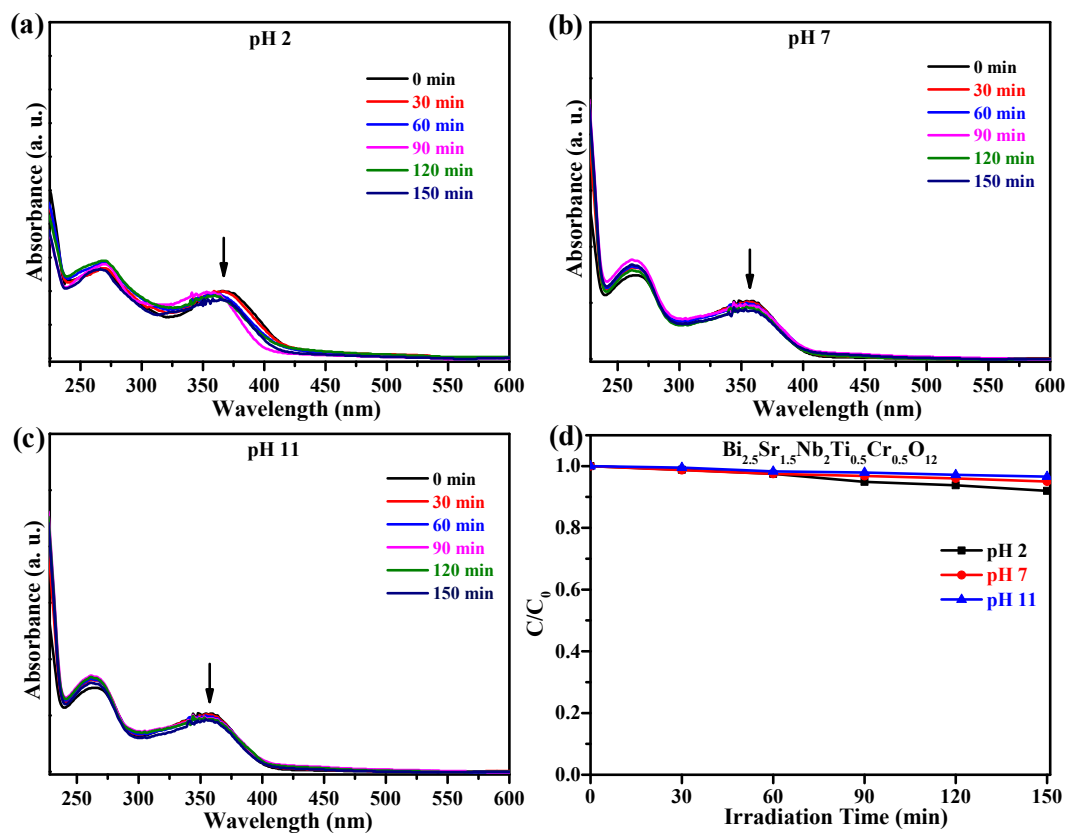


**Fig. S9** UV-vis absorption spectra of TC degradation at (a) pH 2, (b) pH 7 and (c) pH 11 over the catalyst,  $\text{Bi}_{2.5}\text{Sr}_{1.5}\text{Nb}_2\text{Ti}_{0.5}\text{Cr}_{0.5}\text{O}_{12}$  under 150 minutes of light irradiation. (d)  $C/C_0$  plot for TC degradation over the catalyst,  $\text{Bi}_{2.5}\text{Sr}_{1.5}\text{Nb}_2\text{Ti}_{0.5}\text{Cr}_{0.5}\text{O}_{12}$  at different pH values.

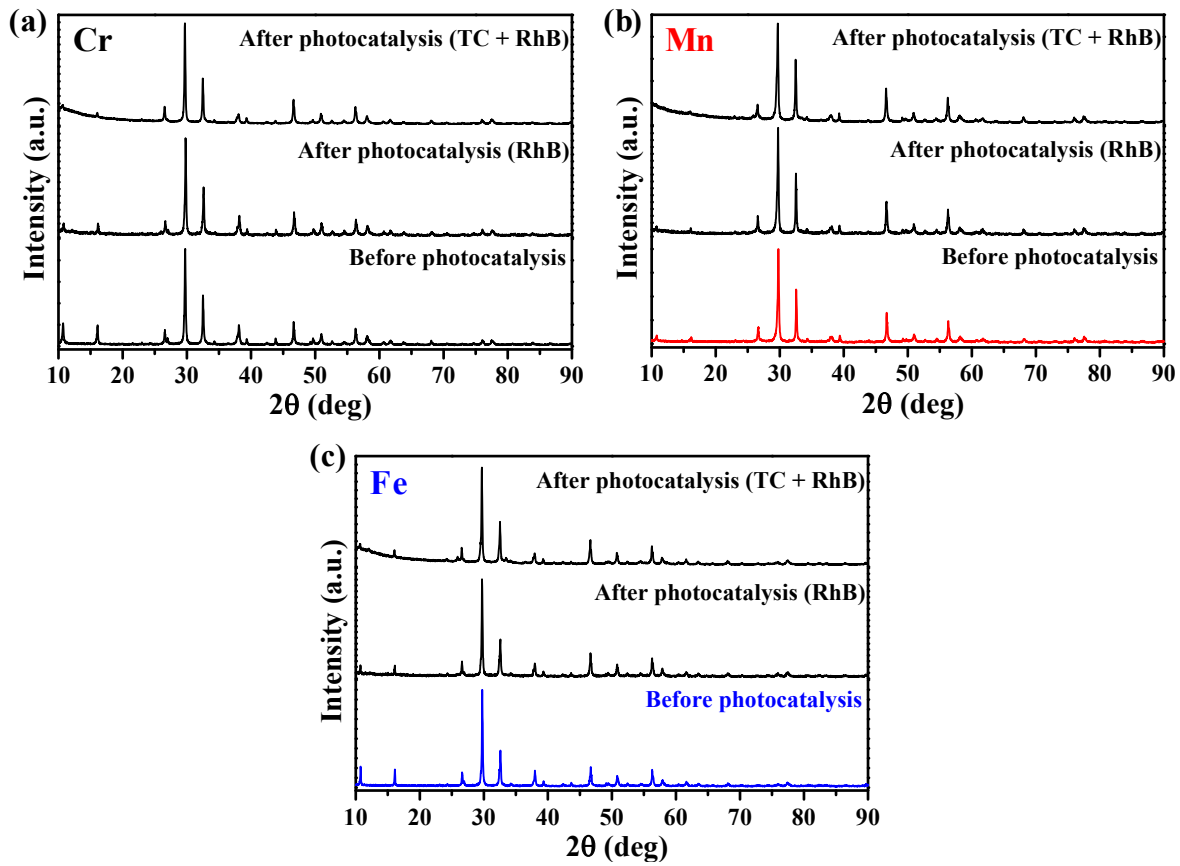


**Fig. S10** PXRD patterns of (a)  $\text{Bi}_{2.5}\text{Sr}_{1.5}\text{Nb}_2\text{Ti}_{0.5}\text{Cr}_{0.5}\text{O}_{12}$ , (b)  $\text{Bi}_{2.5}\text{Sr}_{1.5}\text{Nb}_2\text{Ti}_{0.5}\text{Mn}_{0.5}\text{O}_{12}$  and (c)  $\text{Bi}_{2.5}\text{Sr}_{1.5}\text{Nb}_2\text{Ti}_{0.5}\text{Fe}_{0.5}\text{O}_{12}$  before and after photodegradation of individual RhB and TC-RhB mixture in the acidic medium.

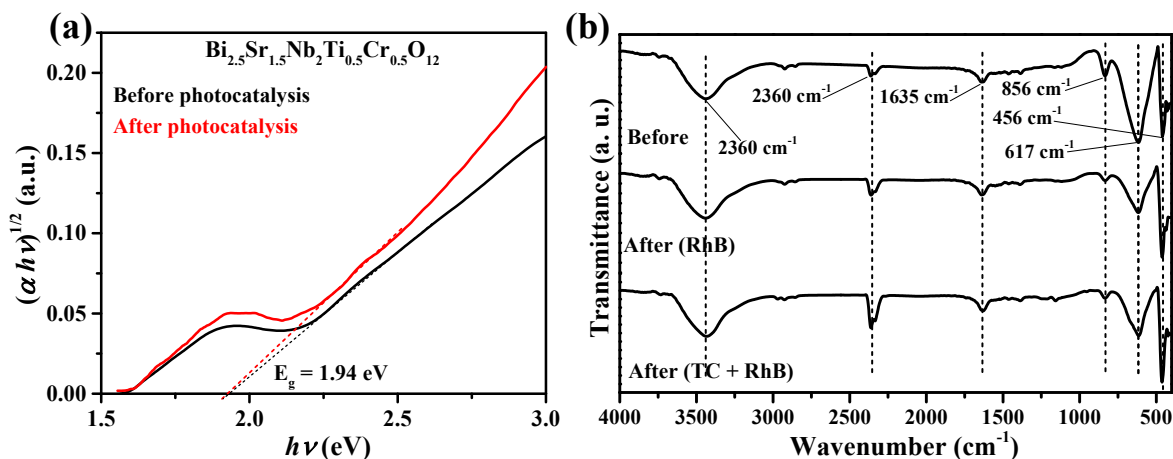


**Fig. S11** Catalyst stability tests of  $\text{Bi}_{2.5}\text{Sr}_{1.5}\text{Nb}_2\text{Ti}_{0.5}\text{Cr}_{0.5}\text{O}_{12}$  with (a) UV-vis DRS and (b) Raman spectroscopy.

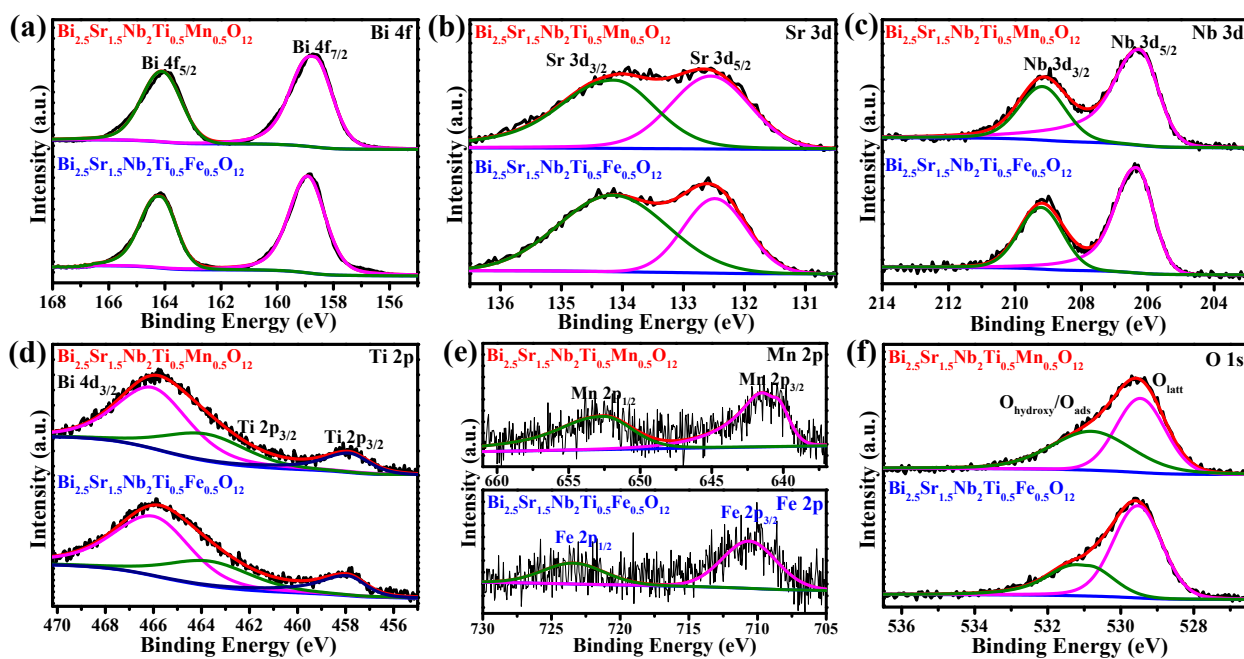


**Fig. S12** High-resolution XPS spectra of (a) Bi 4f, (b) Sr 3d, (c) Nb 3d, (d) Ti 2p, (e) Mn/Fe 2p and (f) O 1s for  $\text{Bi}_{2.5}\text{Sr}_{1.5}\text{Nb}_2\text{Ti}_{0.5}\text{Mn}_{0.5}\text{O}_{12}$  (Mn & Fe).

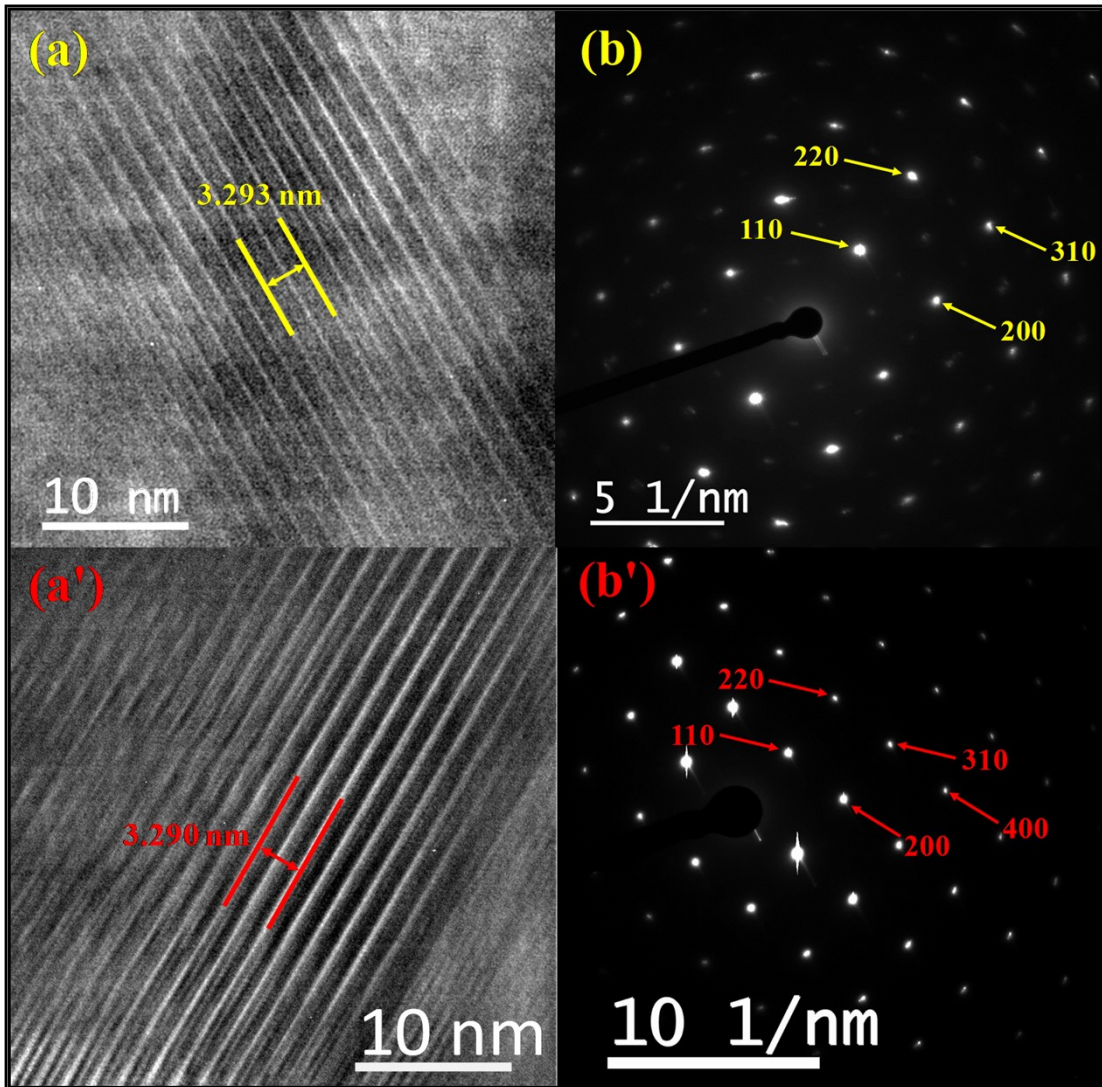


**Fig. S13** HR-TEM (a, a') and SAED pattern (b, b') of  $\text{Bi}_{2.5}\text{Sr}_{1.5}\text{Nb}_2\text{Ti}_{0.5}\text{Cr}_{0.5}\text{O}_{12}$  before (in yellow) and after (in red) photocatalysis.

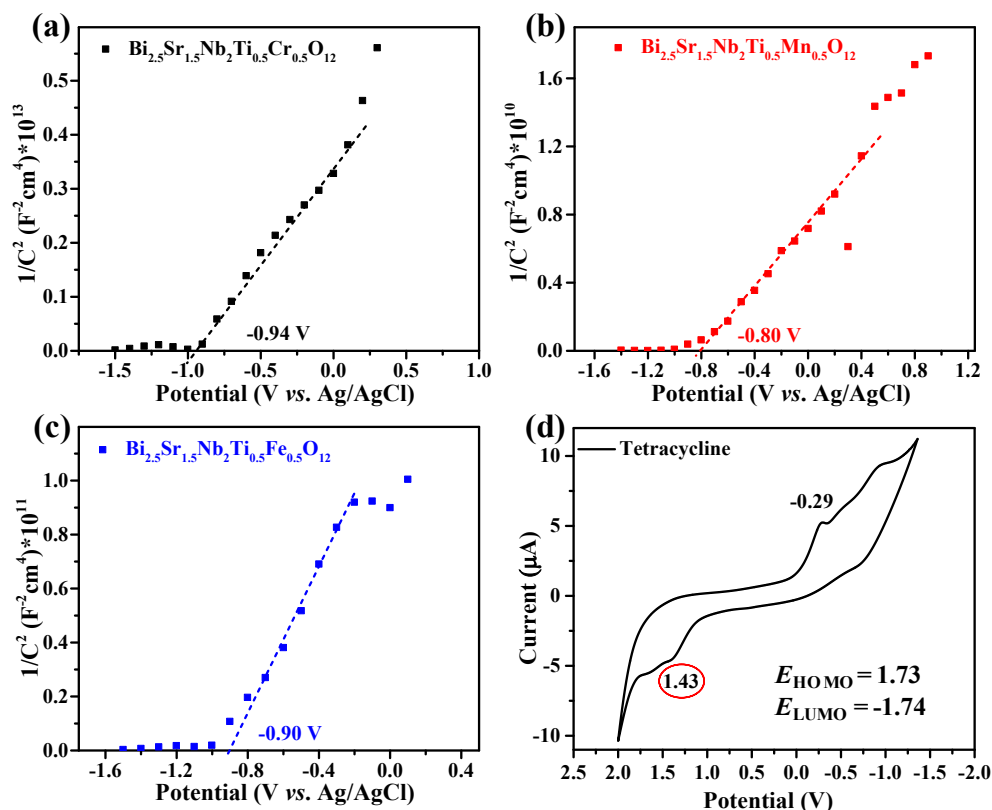


**Fig. S14** (a-c) Mott-Schottky plots of  $\text{Bi}_{2.5}\text{Sr}_{1.5}\text{Nb}_2\text{Ti}_{0.5}\text{M}_{0.5}\text{O}_{12}$  ( $M = \text{Cr}, \text{Mn} \ \& \ \text{Fe}$ ) (recorded at 1 kHz with an amplitude of 10 mV in 0.1 M  $\text{Na}_2\text{SO}_4$  solution of pH = 2.0). (d) Cyclic voltammogram of TC.

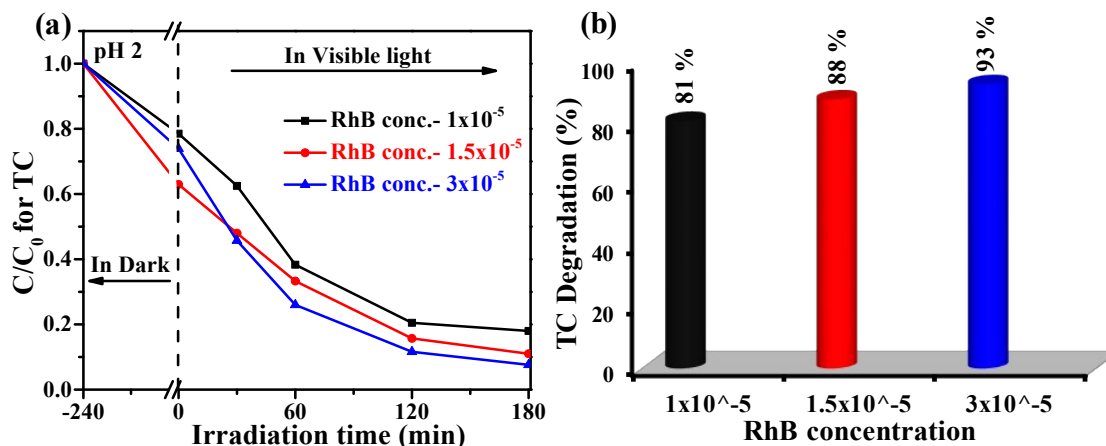


**Fig. S15** (a)  $C/C_0$  plot and (b) bar graph depicting TC degradation from TC-RhB mixture over  $\text{Bi}_{2.5}\text{Sr}_{1.5}\text{Nb}_2\text{Ti}_{0.5}\text{Cr}_{0.5}\text{O}_{12}$  at pH 2 in 180 min of light irradiation with different concentrations of RhB dye.

#### Electron Paramagnetic Resonance (EPR) Measurement:

The role of RhB in the generation of active species was identified by comparing the EPR signal obtained with catalyst suspension in distilled water and in Rhodamine B. The sample for EPR experiment is prepared by dispersing the catalyst powder (10 mg) in 1.5 ml of acidic distilled water (pH 2) followed by the addition of 1.5 ml methanol. Then, 100  $\mu\text{l}$  of prepared suspension is introduced to the EPR tube and analyzed without and with light irradiation (450W xenon lamp). The same procedure was repeated with  $1 \times 10^{-5}$  M RhB solution of pH 2.

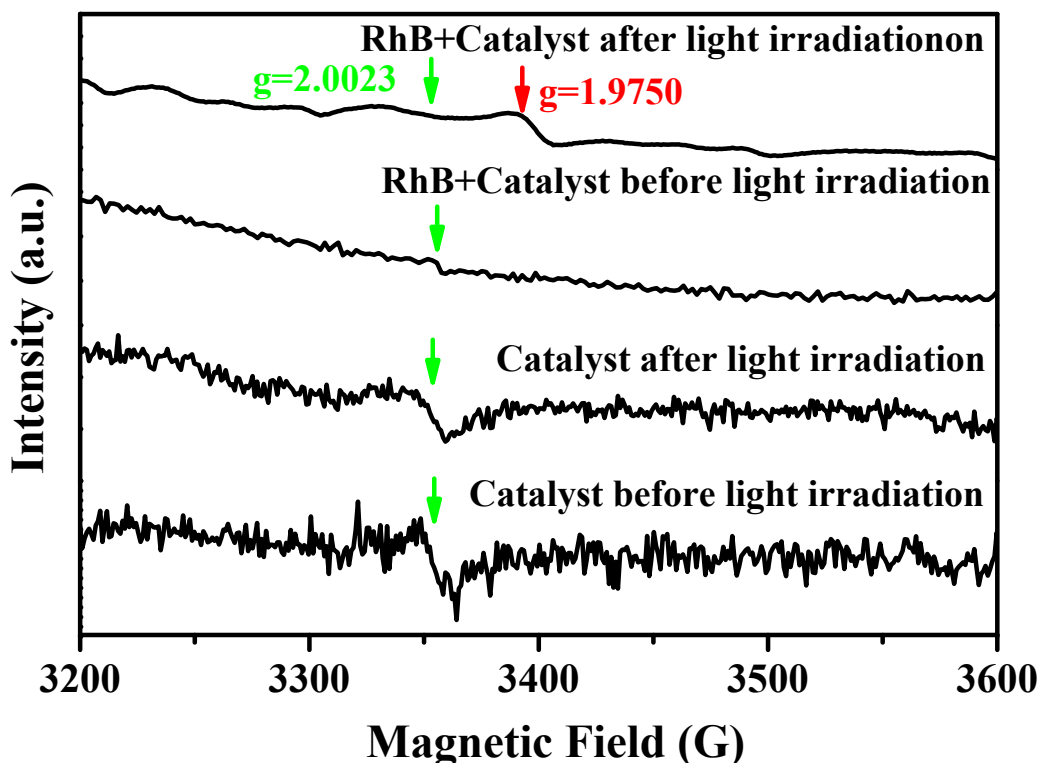


**Fig. S16** EPR spectra of  $\text{Bi}_{2.5}\text{Sr}_{1.5}\text{Nb}_2\text{Ti}_{0.5}\text{Cr}_{0.5}\text{O}_{12}$  (with and without RhB) before and after irradiation by 450 Watt Xenon lamp at 100 K.

